J|A|C|S
ARTICLES
Published on Web 12/02/2006

Nature and Energies of Electrons and Holes in a Conjugated Polymer, Polyfluorene

Norihiko Takeda, Sadayuki Asaoka, and John R. Miller*

Contribution from the Chemistry Department, Brookhaven National Laboratory, Upton, New York 11973-5000

Received April 13, 2006; E-mail: jrmiller@bnl.gov

Abstract: Electrons and holes were injected selectively into poly-2,7-(9,9-dihexylfluorene) (pF) dissolved in a tetrahydrofuran (THF) and a 1,2-dichloroethane (DCE) solution, respectively, using pulse radiolysis. Transient absorption spectra of monoions of both signs revealed two bands attributable to formation of polarons, one in the visible region ($pF^{+\bullet}$ at 580 nm, $pF^{-\bullet}$ at 600 nm) and another in the near-IR region. Additional confirmation for the identification of $pF^{+\bullet}$ and $pF^{-\bullet}$ comes from bimolecular charge-transfer reactions, such as bithiophene$^{-\bullet}$ + pF → pF$^{-\bullet}$ or $pF^{+\bullet}$ + TTA → +$TTA^{+\bullet}$ (TTA = tri-*p*-tolylamine), in which known radical ions transfer charge to pF or from pF. Difference absorption spectra of pF chemically reduced by sodium in THF provided a ratio of absorbance of anions formed to bleaching of the neutral band at 380 nm. In conjunction with pulse-radiolysis results, the data show that each polaron occupies 4.5 ± 0.5 fluorene units, most probably contiguous units. Extensive reduction of pF by sodium also revealed resistance to formation of bipolarons: excess electrons reside as separate polarons when two or more electrons were injected. Redox equilibria with pyrene and terthiophene by pulse radiolysis established reversible one-electron redox potentials of $E^0(pF^{+/0}) = +0.66$ V and $E^0(pF^{0/-}) = -2.65$ V vs $Fc^{+/0}$. Together with the excited-state energy, these results predict a singlet exciton binding energy of 0.2 eV for pF in the presence of 0.1 M tetrabutylammonium tetrafluoroborate. This binding energy would increase substantially without an electrolyte.

Introduction

Conjugated polymers have exciting potential for interconversion of light and electrical energy as organic light-emitting diodes (OLEDs),[1] field-effect transistors (FETs),[2,3] laser materials,[4] sensors,[5] and photovoltaic cells.[6] The emerging field of "Plastic Solar" conjures visions of cheap but highly efficient photovoltaics that utilize properties that can be tailored by organic chemistry.

Realization of the envisaged benefits of these fascinating new materials will require knowledge of their electronic properties. Although separation of electrons and holes is needed for photovoltaics, photoexcitation of conjugated polymers normally produces bound excitons. A goal of this paper is to determine energetics that can predict the excitonic binding energy, information that would be useful in designing materials to separate charge without waste. Intense laser pulses, multiple pulses, or electric fields are reported to dissociate excitons to weakly Coulomb-bound "polaron pairs" or even to free carriers,[7−10] species which are not always clearly distinguished. A second goal of this paper is to provide complete optical signatures of the free carriers that may be used to identify them and to interrogate their natures.

The polymer investigated is polyfluorene (pF), an important blue OLED material.[1] Although the band gap of pure pF is too

(1) Grice, A. W.; Bradley, D. D. C.; Bernius, M. T.; Inbasekaran, M.; Wu, W. W.; Woo, E. P. *Appl. Phys. Lett.* **1998**, *73*, 629−631. Friend, R. H.; Gymer, R. W.; Holmes, A. B.; Burroughes, J. H.; Marks, R. N.; Taliani, C.; Bradley, D. D. C.; Dos Santos, D. A.; Bredas, J. L.; Logdlund, M.; Salaneck, W. R. *Nature* **1999**, *397*, 121−128. Gross, M.; Muller, D. C.; Nothofer, H. G.; Scherf, U.; Neher, D.; Brauchle, C.; Meerholz, K. *Nature* **2000**, *405*, 661−665. Scherf, U.; List, E. J. W. *Adv. Mater.* **2002**, *14*, 477−487.
(2) Chua, L. L.; Zaumseil, J.; Chang, J. F.; Ou, E. C. W.; Ho, P. K. H.; Sirringhaus, H.; Friend, R. H. *Nature* **2005**, *434*, 194−199.
(3) Stutzmann, N.; Friend, R. H.; Sirringhaus, H. *Science* **2003**, *299*, 1881−1884. Ong, B. S.; Wu, Y. L.; Liu, P.; Gardner, S. *J. Am. Chem. Soc.* **2004**, *126*, 3378−3379.
(4) McGehee, M. D.; Gupta, R.; Veenstra, S.; Miller, E. K.; Diaz-Garcia, M. A.; Heeger, A. J. *Phys. Rev. B* **1998**, *58*, 7035−7039. Tessler, N.; Denton, G. J.; Friend, R. H. *Nature* **1996**, *382*, 695−697. Liu, X.; Py, C.; Tao, Y.; Li, Y.; Ding, J.; Day, M. *Appl. Phys. Lett.* **2004**, *84*, 2727−2729.
(5) Swager, T. M. *Acc. Chem. Res.* **1998**, *31*, 201−207. Fan, C. H.; Wang, S.; Hong, J. W.; Bazan, G. C.; Plaxco, K. W.; Heeger, A. J. *Proc. Natl. Acad. Sci. U.S.A.* **2003**, *100*, 6297−6301. Kumaraswamy, S.; Bergstedt, T.; Shi, X. B.; Rininsland, F.; Kushon, S.; Xia, W. S.; Ley, K.; Achyuthan, K.; McBranch, D.; Whitten, D. *Proc. Natl. Acad. Sci. U.S.A.* **2004**, *101*, 7511−7515. Rininsland, F.; Xia, W. S.; Wittenburg, S.; Shi, X. B.; Stankewicz, C.; Achyuthan, K.; McBranch, D.; Whitten, D. *Proc. Natl. Acad. Sci. U.S.A.* **2004**, *101*, 15295−15300. Chen, L. H.; McBranch, D. W.; Wang, H. L.; Helgeson, R.; Wudl, F.; Whitten, D. G. *Proc. Natl. Acad. Sci. U.S.A.* **1999**, *96*, 12287−12292. Nguyen, T. Q.; Wu, J. J.; Doan, V.; Schwartz, B. J.; Tolbert, S. H. *Science* **2000**, *288*, 652−656. Rose, A.; Zhu, Z. G.; Madigan, C. F.; Swager, T. M.; Bulovic, V. *Nature* **2005**, *434*, 876−879.
(6) Yu, G.; Gao, J.; Hummelen, J. C.; Wudl, F.; Heeger, A. J. *Science* **1995**, *270*, 1789−1791. Shaheen, S. E.; Brabec, C. J.; Sariciftci, N. S.; Padinger, F.; Fromherz, T.; Hummelen, J. C. *Appl. Phys. Lett.* **2001**, *78*, 841−843. Wienk, M. M.; Kroon, J. M.; Verhees, W. J. H.; Knol, J.; Hummelen, J. C.; van Hal, P. A.; Janssen, R. A. J. *Angew. Chem., Int. Ed.* **2003**, *42*, 3371−3375. Padinger, F.; Rittberger, R. S.; Sariciftci, N. S. *Adv. Funct. Mater.* **2003**, *13*, 85−88.
(7) Stevens, M. A.; Silva, C.; Russell, D. M.; Friend, R. H. *Phys. Rev. B* **2001**, *63*, 165213.
(8) Nishihara, Y.; Matsuda, A.; Fujii, A.; Ozaki, M.; Frankevich, E. L.; Yoshino, K. *Synth. Met.* **2005**, *154*, 101−104. Tong, M.; Sheng, C. X.; Yang, C.; Vardeny, Z. V.; Pang, Y. *Phys. Rev. B* **2004**, *69*, 155211.
(9) Muller, J. G.; Lemmer, U.; Feldmann, J.; Scherf, U. *Phys. Rev. Lett.* **2002**, *88*. Muller, J. G.; Lupton, J. M.; Feldmann, J.; Lemmer, U.; Scharber, M. C.; Sariciftci, N. S.; Brabec, C. J.; Scherf, U. *Phys. Rev. B* **2005**, *72*.
(10) Dyakonov, V.; Frankevich, E. *Chem. Phys.* **1998**, *227*, 203−217.

Scheme 1. Synthesis of Poly-2,7-(9,9-dihexylfluorene)

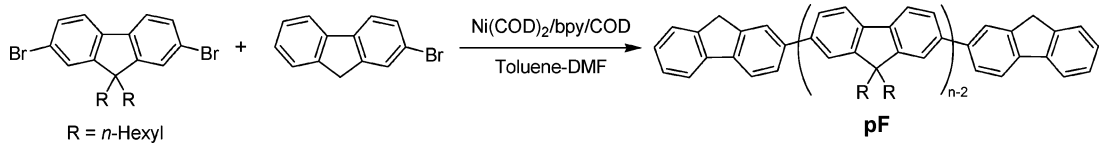

wide for it to function alone to efficiently produce energy from sunlight, derivatives of pF and pFs in combination with other materials find consideration as solar materials.[11] This paper will seek basic information about the form that electrons and holes take in conjugated fluorenes to understand how the natures of these charges affect their mobilities, a key property that makes conjugated materials exciting. Single charges in conjugated polymers are partly "self-trapped" by the deformations they create in polar molecular material but may be mobile as "polarons", which carry these deformations with them as they move. The high mobilities[2,12] and "wirelike" behavior in a charge transfer[13] are critical for efficient solar energy conversion. Early interpretations of data finding that spin concentrations first increased, but then decreased, with increased doping identified pairs of like charges occupying the same region of space called "bipolarons" as the principle form of charges in conjugated polymers.[14] Recent findings favor polarons[15−19] as the more stable species. Although questions remain for polyfluorene,[20,21] this paper will seek to understand especially the electrons.

Earlier experiments have partially illuminated the energetics, but accurate information has been difficult to obtain because electrochemical experiments often do not succeed to obtain reversible, thermodynamic potentials.[13,15,22−24] Goldsmith[13] obtained redox potentials for short oligomers of fluorene, F_n, with $n = 1-3$, but the measurements failed for oligomers with more than 3 units. Approximate redox potentials have been reported for pFs both in solution[23] and in solid films on electrodes;[22] however, both studies suffered from irreversibilities in cyclic voltammograms or hysteresis typical for solid states,[25] and the data were not in complete agreement with each other. For a spirofluorene polymer, Laquai[26] reported a broad but reversible CV giving $E^0(pF^{+\bullet}/pF) = +0.46$ V vs Fc/Fc^+.

This paper describes spectroscopic measurements of electrons and holes injected into polyfluorene either chemically or through the use of short electron pulses in experiments having an ~1 ns time resolution. At short times, the experimental conditions definitively identify the spectra associated with injection of single electrons or holes into pF, which compare to those at longer times. The measurements obtain the number of fluorene units (delocalization length) occupied by a charge and observe bimolecular charge-transfer equilibria yielding reversible potentials for both electron and hole injection into pF. The experiments are conducted in solution where the polymers exist dominantly as single strands, an aspect also examined by the time-resolved experiments.

Experimental Section

Chemicals. Biphenyl (Fischer) was zone-refined in ambient air (or recrystallized 4× from ethanol). Benzophenone (Aldrich, 99+%), pyrene (Fluka, puriss, ≥99%), and terthiophene (Aldrich) were zone-refined in ambient air. Bithiophene (Aldrich) was vacuum sublimed. 1,2-Dichloroethane (Aldrich) was stored over molecular sieves 3 Å and 5 Å. Ferrocene (Alfa, recrystallized) was sublimed, and tri-*p*-tolylamine (Aldrich, 97%) was recrystallized from absolute ethanol and sublimed under a vacuum. Nitrobenzene (Aldrich) was used as received; tetrabutylammoniumtetrafluoroborate (Bu_4NBF_4, Fluka, electrochemical grade) was recrystallized from ethylacetate and dried under a vacuum at 80 °C. Tetrahydrofuran (Aldrich, anhydrous, inhibitor free) was distilled from sodium-benzophenone ketyl under argon. Toluene and *N*,*N*-dimethylformamide (DMF) were fractionally distilled under an argon atmosphere from sodium and calcium hydride, respectively, and then degassed through freeze−pump−thaw cycles. 2-Bromofluorene, bis(1,5-cyclooctadiene) nickel(0), 1,5-cyclooctadiene, and 2,2′-bipyridine were used as purchased from Aldrich. A 2,7-dibromo-9,9-dihexylfluorene monomer was prepared from 2,7-dibromofluorene (Aldrich) according to the procedure reported by Tsolakis et al.[27] ^{1}H NMR: $\delta_H(CDCl_3)$ 7.51 (m, 2H), 7.45 (m, 4H), 1.91 (m, 4H), 1.10 (m, 4H), 1.03 (m, 8H), 0.78 (t, $J = 7.1$ Hz, 6H), 0.58 (m, 4H). ^{13}C NMR: $\delta_C(CDCl_3)$ 152.8, 139.3, 130.4, 126.4, 121.7, 121.3, 55.9, 40.4, 31.7, 29.8, 23.9, 22.8, 14.2. Water was purified by a Milli-Q water purification system (18 M Ω cm^{-1}).

Synthesis of Poly-2,7-(9,9-dihexylfluorene) (pF). The pF was prepared by polycondensation of 2,7-dibromo-9,9-dihexylfluorene according to the procedure reported by Klaerner et al.,[28] as shown in Scheme 1. To control the averaged molecular weight, 2-bromofluorene was used as the end-capping reagent: In a Schlenk tube, bis(1,5-cyclooctadiene) nickel(0) (1.8 mmol), 1,5-cyclooctadiene (1.8 mmol),

(11) Ramsdale, C. M.; Barker, J. A.; Arias, A. C.; MacKenzie, J. D.; Friend, R. H.; Greenham, N. C. *J. Appl. Phys.* **2002**, *92*, 4266−4270. Kietzke, T.; Neher, D.; Kumke, M.; Montenegro, R.; Landfester, K.; Scherf, U. *Macromolecules* **2004**, *37*, 4882−4890. Snaith, H. J.; Greenham, N. C.; Friend, R. H. *Adv. Mater.* **2004**, *16*, 1640−1645. Wang, X. J.; Perzon, E.; Delgado, J. L.; de la Cruz, P.; Zhang, F. L.; Langa, F.; Andersson, M.; Inganas, O. *Appl. Phys. Lett.* **2004**, *85*, 5081−5083. Demadrille, R.; Firon, M.; Leroy, J.; Rannou, P.; Pron, A. *Adv. Funct. Mater.* **2005**, *15*, 1547−1552. Tian, R. Y.; Yang, R. Q.; Peng, J. B.; Cao, Y. *Chin. Phys.* **2005**, *14*, 1032−1035.
(12) Warman, J. M.; de Haas, M. P.; Dicker, G.; Grozema, F. C.; Piris, J.; Debije, M. G. *Chem. Mater.* **2004**, *16*, 4600−4609. Grozema, F. C.; Savenije, T. J.; Vermeulen, M. J. W.; Siebbeles, L. D. A.; Warman, J. M.; Meisel, A.; Neher, D.; Nothofer, H. G.; Scherf, U. *Adv. Mater.* **2001**, *13*, 1627−1630. Grozema, F. C.; Siebbeles, L. D. A.; Warman, J. M.; Seki, S.; Tagawa, S.; Scherf, U. *Adv. Mater.* **2002**, *14*, 228−231.
(13) Goldsmith, R. H.; Sinks, L. E.; Kelley, R. F.; Betzen, L. J.; Liu, W. H.; Weiss, E. A.; Ratner, M. A.; Wasielewski, M. R. *Proc. Natl. Acad. Sci. U.S.A.* **2005**, *102*, 3540−3545.
(14) Nowak, M. J.; Rughooputh, S.; Hotta, S.; Heeger, A. J. *Macromolecules* **1987**, *20*, 965−968. Nowak, M. J.; Spiegel, D.; Hotta, S.; Heeger, A. J.; Pincus, P. A. *Macromolecules* **1989**, *22*, 2917−2926.
(15) Chen, X. W.; Inganas, O. *J. Phys. Chem.* **1996**, *100*, 15202−15206.
(16) Furukawa, Y. *J. Phys. Chem.* **1996**, *100*, 15644−15653.
(17) Guay, J.; Diaz, A.; Wu, R. L.; Tour, J. M.; Dao, L. H. *Chem. Mater.* **1992**, *4*, 254−255. Hoier, S. N.; Park, S. M. *J. Phys. Chem.* **1992**, *96*, 5188−5193.
(18) van Haare, J.; Havinga, E. E.; van Dongen, J. L. J.; Janssen, R. A. J.; Cornil, J.; Bredas, J. L. *Chem.−Eur. J.* **1998**, *4*, 1509−1522.
(19) Yokonuma, N.; Furukawa, Y.; Tasumi, M.; Kuroda, M.; Nakayama, J. *Chem. Phys. Lett.* **1996**, *255*, 431−436.
(20) Greczynski, G.; Fahlman, M.; Salaneck, W. R. *J. Chem. Phys.* **2000**, *113*, 2407−2412.
(21) Fung, M. K.; Lai, S. L.; Bao, S. N.; Lee, C. S.; Lee, S. T.; Wu, W. W.; Inbasekaran, M.; O'Brien, J. J. *J. Vac. Sci. Technol., A* **2002**, *20*, 911−918.
(22) Janietz, S.; Bradley, D. D. C.; Grell, M.; Giebeler, C.; Inbasekaran, M.; Woo, E. P. *Appl. Phys. Lett.* **1998**, *73*, 2453−2455.
(23) Miteva, T.; Meisel, A.; Knoll, W.; Nothofer, H. G.; Scherf, U.; Muller, D. C.; Meerholz, K.; Yasuda, A.; Neher, D. *Adv. Mater.* **2001**, *13*, 565−570.
(24) Funston, A. M.; Silverman, E. E.; Miller, J. R.; Schanze, K. S. *J. Phys. Chem. B* **2004**, *108*, 1544−1555.
(25) Meerholz, K.; Heinze, J. *Electrochim. Acta* **1996**, *41*, 1839−1854.
(26) Laquai, F.; Wegner, G.; Im, C.; Bassler, H.; Heun, S. *J. Appl. Phys.* **2006**, *99*, 023712.
(27) Tsolakis, P. K.; Kallitsis, J. K. *Chem.−Eur. J.* **2003**, *9*, 936−943.
(28) Klaerner, G.; Miller, R. D. *Macromolecules* **1998**, *31*, 2007−2009.

and 2,2′-bipyridine (1.8 mmol) were dissolved in the mixed solvent of toluene (12 mL) and DMF (12 mL) and heated at 80 °C for 30 min under an argon atmosphere. A toluene solution (8 mL) of 2,7-dibromo-9,9-dihexylfluorene (1.0 mmol) and 2-bromofluorene was added, and the reaction mixture was heated at 80 °C for 12 h then poured into an equivolume mixture of concentrated hydrochloric acid, methanol, and acetone. The organic layer was extracted with toluene, washed with brine, and then dried over sodium sulfate. The solvent was removed under reduced pressure, and the crude polymer was dissolved in a small amount of chloroform and reprecipitated twice from methanol prior to Soxhlet extraction with acetone for 3 days to remove low molecular weight oligomers. ^{1}H NMR: $\delta_H(CDCl_3)$ 7.92−7.30 (m, 6H), 4.02 (s, 0.117H, 9-H of terminal fluorenes), 2.38−1.85 (m, 4H), 1.33−1.00 (m, 12H), 0.95−0.62 (m, 10H).

The number-averaged molecular weight (M_n) and polydispersity (M_W/M_N) of pF were determined on GPC by using polystylene calibration standards (Aldrich): $M_N = 5930$, $M_W/M_N = 1.60$. To obtain a more accurate calibration, a series of oligofluorenes with 1−8 fluorene units were synthesized according to the modified procedures reported by Geng et al.[29] Apparent molecular weights calculated from GPC elution volumes based on polystylene standards afforded an excellent linear relationship ($R^2 = 0.9985$) to the actual molecular weights. $M_N = 3280$ was obtained for pF using the oligofluorene standard. End capping by unalkylated fluorene was only one-third complete as indicated by the observed ratio of 34.2 protons on α-carbons of hexyl groups (2.38−1.85 ppm) to those on 9-positions of terminal fluorenes (4.02 ppm) vs the expected 43.6/4 = 10.9. These observations point to an average of 10.9 ($n \sim 11$) fluorene units per polymer. Although pF was produced by a polymer synthesis and is polydisperse, its short length is typical of oligomers.[28]

^{1}H NMR spectra were obtained on a Bruker 400 MHz spectrometer in chloroform-*d*. Gel permeation chromatography (GPC) analysis of pF was carried out on a 300 × 7.5 mm KF-803L (Shodex) and a 300 × 7.5 mm, 6 μ TSK gel column (Tosoh) equipped with an ERC-7520 RI detector (Erma) using THF as eluent. Stationary absorption spectra were recorded using a Cary 5 UV−vis−NIR spectrophotometer (Varian Instruments). Cyclic voltammograms in THF (0.1 M Bu_4NBF_4 as supporting electrolyte) were recorded on a BAS100B electrochemical analyzer. A Pt disk and a Pt wire served as a working and a counter electrode, respectively, and Ag/Ag^+ in acetonitrile was used as a reference electrode. Potentials were calibrated using ferrocene as an internal standard.

Time-Resolved Experiments. This work was carried out at the Brookhaven National Laboratory Laser-Electron Accelerator Facility (LEAF)[30] which produces electron pulses as short as 5 ps. For the present experiments, pulses ≤50 ps duration were focused into quartz cells with high-purity silica windows containing argon-saturated solutions.

The electron pulses pass completely through and exit the cells, creating ionization events. These ionizations lead to formation of $pF^{-\bullet}$ in THF or $pF^{+\bullet}$ in 1,2-dichloroethane (DCE). In THF, abbreviated as RH, and in DCE, abbreviated here as RCl, the principal reactions in solutions containing pF as a dilute solute are:

$$RH \rightarrow RH^{+\bullet} + e_s^- \quad \text{(ionization)}$$

$$RH^{+\bullet} + RH \rightarrow RH_2^+ + R^\bullet \quad \text{(proton transfer to neighbor)}$$

$$pF + e_s^- \rightarrow pF^{-\bullet} \quad \text{(electron attachment to pF)}$$

$$RCl \rightarrow RCl^{+\bullet} + e^- \quad \text{(ionization)}$$

$$e^- + RCl \rightarrow R^\bullet + Cl^- \quad \text{(electron scavenged by solvent)}$$

$$pF + RCl^{+\bullet} \rightarrow pF^{+\bullet} + RCl \quad \text{(hole attachment to pF)}$$

In both cases, the first step is ionization, predominantly of solvent molecules, to create radical cations and electrons. In THF, the cations quickly (<10 ps) transfer protons to create solvated protons and radicals, which do not react with pF; in DCE, the electrons are very rapidly transformed into unreactive Cl^- and radicals. Electrons in THF then reduce pF, and holes in DCE oxidize pF. These species were detected by their transient absorption spectra as described further in the Experimental Details section.

In early times, especially in THF, emission was observed in the blue (∼380−460 nm), ascribed to the excited states of pF with lifetimes of ∼3 ns. The reported transient absorptions are corrected for these emissions where necessary. The excited-state formation is probably due to absorption of Cerenkov radiation and/or energy transfer from the excited solvents.

Results

Formation and Spectra of $pF^{-\bullet}$ Anions and $pF^{+\bullet}$ Cations. Figure 1 shows kinetic traces for the formation of $pF^{+\bullet}$ in DCE (at 580 nm) and $pF^{-\bullet}$ in THF (at 600 nm) created by electron pulses at LEAF along with absorption due to solvent cations in neat DCE and electrons in neat THF. The $pF^{+\bullet}$ spectrum is similar to that reported by Burrows[31] but extends further into the near-infrared region. Single-exponential fits over a 10-fold

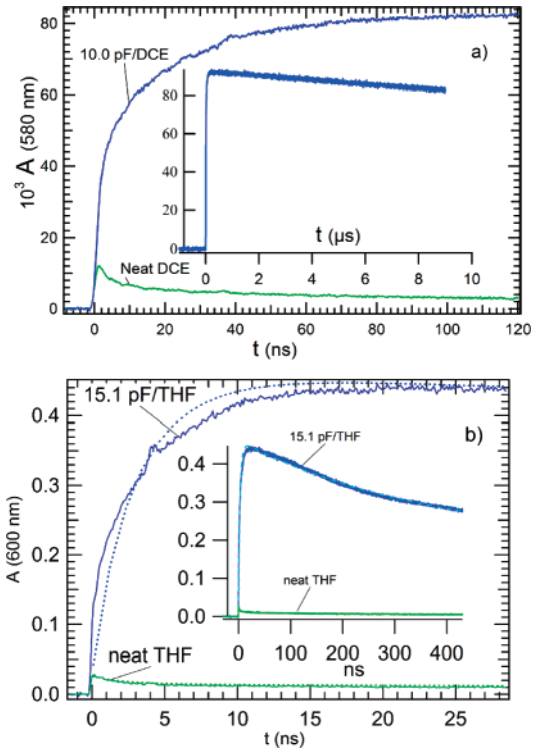

Figure 1. Kinetic traces for formation of $pF^{+\bullet}$ in DCE (a) and $pF^{-\bullet}$ in THF (b) along with fits shown as dashed lines. To illustrate nonexponential kinetics attributed to transient terms in the diffusion equations, the dashed line shows a fit to the $pF^{-\bullet}$ growth that is based on the (false) assumption that single-exponential charge-transfer kinetics to pF occurs in competition with the decay of solvent electrons or holes. Although the dashed line itself departs from single-exponential due to that competition, the much greater departure of the $pF^{-\bullet}$ growth is evident. pF concentrations are in millimolars of the monomer.

(29) Geng, Y. H.; Trajkovska, A.; Katsis, D.; Ou, J. J.; Culligan, S. W.; Chen, S. H. *J. Am. Chem. Soc.* **2002**, *124*, 8337−8347.
(30) Wishart, J. F. In *Radiation Chemistry: Present Status and Future Trends;* Jonah, C. D., Rao, B. S. M., Eds.; Elsevier Science: Amsterdam, 2001; Vol. 87, pp 21−35. Wishart, J. F.; Cook, A. R.; Miller, J. R. *Rev. Sci. Instrum.* **2004**, *75*, 4359−4366.

range of concentrations gave rate constants for hole attachment in DCE of ~4.5 × 10^9 M^{-1} s^{-1} per monomer or of 5.0 × 10^{10} M^{-1} s^{-1} per polymer molecule (n = 11) and for electron attachment in THF of 2.6 × 10^{10} M^{-1} s^{-1} (per monomer) or of 2.9 × 10^{11} M^{-1} s^{-1} (per polymer). These rate constants were evaluated from the slower portions of the rise of $pF^{+\bullet}$ and $pF^{-\bullet}$, neglecting fast contributions (see below). Electron attachment is faster in THF due to faster diffusion of solvated electrons in that fluid. Lifetimes of ions were about 10 μs in THF, and those in DCE were much longer. These observations indicate that in THF, $pF^{-\bullet}$ ions react rapidly with their counterions, solvated protons (RH_2^+), but in DCE, $pF^{+\bullet}$ ions do not react with their Cl^- counterions. The lack of reaction of $pF^{+\bullet}$ ions with Cl^- is consistent with recent findings from this laboratory.[32]

The rate constants for electron and hole attachment to pF (per polymer) are only about three times larger than the values measured here for charge attachment to biphenyl: 7.4 × 10^{10} M^{-1} s^{-1} for electron attachment in THF[33]and ~1.7 × 10^{10} M^{-1} s^{-1} for hole attachment in DCE. The rate for biphenyl in THF found here is midway between those[33] reported by Dorfman[34] and by Renou;[35] the rate in DCE is similar to a recent report from this lab.[32] Although pF is 11 times longer than biphenyl, electron and hole attachment rate constants to pF are larger by only a factor of 3. This is expected for diffusion-controlled reactions, as understood by Traytak's theory,[36] which has been qualitatively confirmed in application to reactions with conjugated polymers.[24,37]

The Traytak theory also predicts large transient terms, the effects of which are evident in the growth of pF ions in Figure 1, which markedly depart from single-exponential time dependence at short times. Traytak's theory[36,37] describes how transient terms in the Smoluchowski equation[38] are larger and persist longer for large molecules such as conjugated polymers. The transient terms give faster capture at short times. Although in Figure 1b the best exponential fit gives $\tau = 1/k = 3.8$ ns, more than half of the $pF^{-\bullet}$ has been formed before 1 ns. Markedly, nonexponential charge capture by long conjugated molecules was reported earlier.[24,37] The present data do not quantitatively test predictions of the Traytak theory. The data do confirm that the expected diffusion-controlled rates (slower part) are preceded by fast capture that appears consistent with the theory.

Figure 2 displays transient absorption spectra of polyfluorene anions and cations overlaid on the spectrum of chemically reduced pF in THF. Absorption spectra of $pF^{-\bullet}$ at 300 ns in THF and of $pF^{+\bullet}$ at 1.0 μs in DCE are reported as molar extinction coefficients (Table 1). Concentrations of anions and cations, both near 1 μM, were determined by taking measurements on species having known extinction coefficients under the same conditions. Reference extinction coefficients (M^{-1} cm^{-1}) were ϵ(benzophenone$^{-\bullet}$, 754 nm) = 8.5 × 10^3 [39] and ϵ(e_s^-, 2120 nm) = 4.0 × 10^4 [34,40] for determination of ϵ($pF^{-\bullet}$) and ϵ_{670}(tritolylamine$^{+\bullet}$) = 2.75 × 10^4 [41] for determination of ϵ($pF^{+\bullet}$).

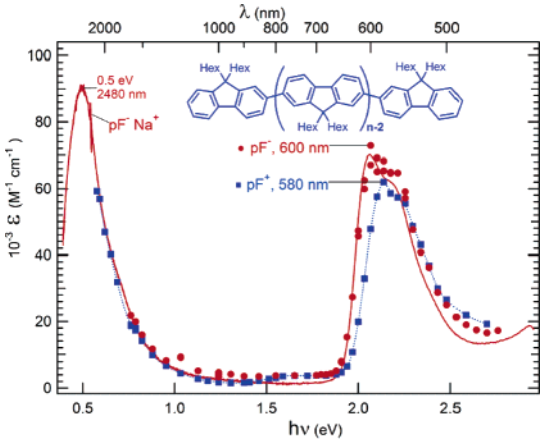

Figure 2. Transient absorption spectra of anions of polyfluorene ($pF^{-\bullet}$) in THF or cations of polyfluorene ($pF^{+\bullet}$) in DCE produced by electron pulses. The spectrum of $pF^{-\bullet}$ produced in THF reduced by Na metal is nearly identical. The dotted blue line is interpolated through the $pF^{+\bullet}$ spectrum.

Table 1. Molar Extinction Coefficients (M^{-1} cm^{-1}) for Polyfluorene (pF) and Its Ions Reported Per Monomer Unit for the Neutral and Per Ion for $pF^{-\bullet}$ and $pF^{+\bullet}$[a]

ϵ_{382}(pF)[b]	ϵ_{600}($pF^{-\bullet}$)	ϵ_{382}($pF^{-\bullet}$)[c]	ϵ_{580}($pF^{+\bullet}$)
(3.4 ± 0.1) × 10^4 $dA_{382}/d[pF_1]$	(7.0 ± 0.7) × 10^4 $dA_{600}/d[pF^{-\bullet}]$	(1.0 ± 0.6) × 10^4 $dA_{382}/d[pF^{-\bullet}]$	(6.2 ± 0.6) × 10^4 $dA_{580}/d[pF^{+\bullet}]$

[a] Also shown are their identifications as differentials of the absorbance at the unit path length. [b] Extinction coefficient per monomer unit, with the derivative of absorbance at 382 nm per monomer unit. [c] Estimated from absorption when all the neutral has been removed (spectrum 7 in Figure 3). Substantial uncertainty occurs because interactions between densely packed anions may distort the spectra.

$pF^{-\bullet}$ Polarons by Chemical Reduction with Sodium. Figure 3 shows difference absorption spectra during chemical reduction of polyfluorene to $pF^{-\bullet}$ by repeated contacts with Na metal in THF. Visible (2.07 eV, 600 nm) and near IR bands (0.5 eV, 2480 nm) produced in the early stages of Na reduction are similar to those from reduction with electron pulses in THF; spectrum 3 is also plotted in Figure 2 to facilitate comparison. The spectra in Figure 3 also measure the removal (bleach) of the pF neutral band at 380 nm. First contacts with Na *increased* this neutral pF band (spectrum 1), and no bands of the anion appeared. Possible reasons for this unexpected increase include (1) reduction of impurities, (2) fluorene carbanion formation at end caps, (3) anions reacting with trace amounts of water to produce H adducts, and (4) Na adducts produced from reaction of Na with the end-phenyl ring (sodium-fluorene). After the series of contacts with Na, exposure to air removed the anion bands leaving a yellow color.[42]

In later stages of the reductions, the pF neutral band at 380 nm was entirely removed (spectrum 7), as is most clearly seen in inset (a) of Figure 3, which plots absorption spectra in the

(31) Burrows, H. D.; de Melo, J. S.; Forster, M.; Guntner, R.; Scherf, U.; Monkman, A. P.; Navaratnam, S. *Chem. Phys. Lett.* **2004**, *385*, 105−110.
(32) Funston, A. M.; Miller, J. R. *Radiat. Phys. Chem.* **2005**, *72*, 601−611.
(33) Dorfman found 1 × 10^{11} M^{-1} s^{-1}, and Renou found 4 × 10^{10} M^{-1} s^{-1}.
(34) Jou, F. Y.; Dorfman, L. M. *J. Chem. Phys.* **1973**, *58*, 4715−4723.
(35) Renou, F.; Archirel, P.; Pernot, P.; Levy, B.; Mostafavi, M. *J. Phys. Chem. A* **2004**, *108*, 987−995.
(36) Traytak, S. D. *Chem. Phys. Lett.* **1992**, *197*, 247−254. Traytak, S. D. *Chem. Phys. Lett.* **1994**, *227*, 180−186.
(37) Grozema, F. C.; Hoofman, R.; Candeias, L. P.; de Haas, M. P.; Warman, J. M.; Siebbeles, L. D. A. *J. Phys. Chem. A* **2003**, *107*, 5976−5986.
(38) Smoluchowski, M. *Z. Phys.* **1916**, *17*, 557−571.
(39) Pedersen, S. U.; Christensen, T. B.; Thomasen, T.; Daasbjerg, K. *J. Electroanal. Chem.* **1998**, *454*, 123−143.
(40) Dorfman, L. M.; Jou, F. Y.; Wageman, R. *Ber. Bunsen-Ges. Phys. Chem.* **1971**, *75*, 681−685.
(41) Pedersen, L.; Pedersen, S. U., private communication.
(42) Visual changes during reduction were not observed in this experiment, but in other reductions, samples appeared yellow in the early stages. This might be due to absorbance changes or to loss of (blue) fluorescence.

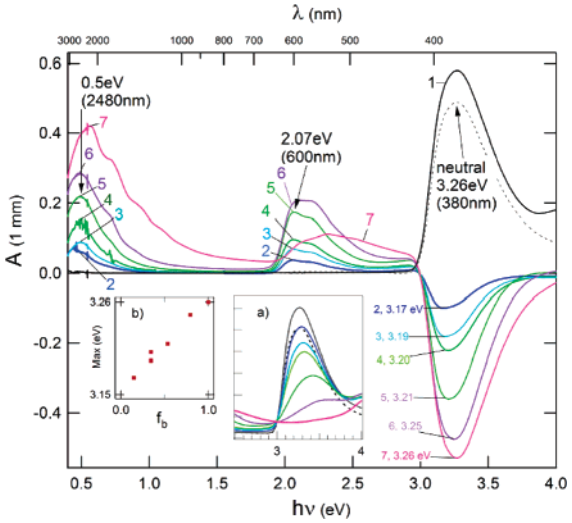

Figure 3. Absorption spectra of 0.14 mM (monomer units) polyfluorene (pF) reduced by Na metal in THF. The dashed line shows the absorption band of neutral pF at 380 nm before contact with Na. Spectrum 1 has an increased absorption at 380 nm but no anion bands. Spectra 2−7 formed on successive exposures to Na are shown as differences relative to spectrum 1. In spectrum 7, the neutral band is completely bleached, as can also be seen in inset (a), which plots simple absorption spectra (not differences). Inset (b) plots the maximum of the band bleached vs the fraction bleached.

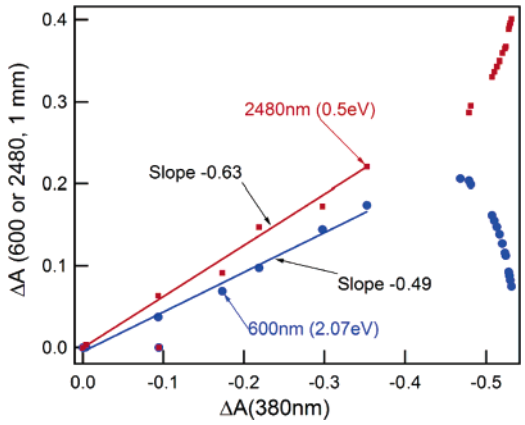

Figure 4. Creation of $pF^{-\bullet}$ absorbance at 600 and 2480 nm as a function of the bleach of neutral pF absorbance at 380 nm during reduction by Na in THF. Path = 1 mm.

region of the neutral bleaching. Inset (b) plots the maximum energy of the bleached band as a function of the fraction bleached, f_b, estimated from oscillator strengths in the neutral region (3.0−3.92 eV), assuming that spectrum 7 arises entirely from anions. The position of the band bleached shifts to higher energy with increased bleaching, f_b.

Although the bleached neutral band shifts, the absorption maxima of the anion at 0.5 and 2.07 eV change little through spectrum 6, where 80% of the neutral has been bleached, as judged by the loss of the neutral band. The heights of these two anion bands increase linearly with the decrease of neutral absorption as seen in Figure 4. The slope of the lines in Figure 4 can be used to estimate how many monomer units were bleached when one charge was injected into a pF chain. Equation 1 assumes that injection of an electron (or hole) into a polymer creates an ion, which occupies l_n monomer units, and that those monomer units no longer have the properties of the ground-state neutral. If f_1 refers to one monomer unit (one fluorene in this case):

$$l_n = -\mathrm{d}[f_1]/\mathrm{d}[\mathrm{ion}] \tag{1}$$

The postulate of eq 1 is general and can be applied to production of anions, cations, or singlet or triplet excited states delocalized over l_n monomer units. Equation 2 (derived in the Supporting Information) obtains the delocalization length, $l_n = 4.5 \pm 0.5$, for $pF^{-\bullet}$; absorbance from 4.5 monomer (f_1) units is bleached when one anion is created. In Equation 2, the ratio of the absorbance bleach at the neutral band (382 nm) to the absorbance growth at the anion band (600 nm) is converted into a ratio of neutral loss per anion created using the appropriate extinction coefficients. Table 1 gives the extinction coefficients and identifies them with the terms in eq 2. Equation 2 includes corrections to observed absorbance values for absorption tails of the anion at the maximum of the neutral, which requires knowledge of the extinction coefficient of the anion at λ_{max} of the neutral. This was estimated from the absorbance in spectrum 7, Figure 3, but the high anion concentrations may have produced distortions. Therefore, this second term in the denominator of eq 2 is a principle source of the stated uncertainty in the determination of the delocalization length. The corresponding term in the numerator, $\epsilon_{600}(\mathrm{pF})$, is zero.

$$l_n = \frac{\mathrm{d}A_{382}}{\mathrm{d}A_{600}} \frac{\dfrac{\mathrm{d}A_{600}}{\mathrm{d}[\mathrm{pF}^{-\bullet}]} - l_n \dfrac{\mathrm{d}A_{600}}{\mathrm{d}[\mathrm{pF}_1]}}{\left[-\dfrac{\mathrm{d}A_{382}}{\mathrm{d}[\mathrm{pF}_1]} + \dfrac{1}{l_n} \dfrac{\mathrm{d}A_{382}}{\mathrm{d}[\mathrm{pF}^{-\bullet}]} \right]}$$

$$= -\frac{\mathrm{d}A_{382}}{\mathrm{d}A_{600}} \frac{\epsilon_{600}(\mathrm{pF}^{-\bullet}) - l_n \epsilon_{600}(\mathrm{pF})}{\epsilon_{382}(\mathrm{pF}_1) - \dfrac{1}{l_n} \epsilon_{382}(\mathrm{pF}^{-\bullet})} \tag{2}$$

The rise of absorbance in Figure 4 remains linear until $\Delta A_{382} = \sim -0.45$, where the visible (600 nm) band of the anion abruptly begins to decrease and the increase of the near IR band becomes steeper. This end of linearity point corresponds closely to spectrum 6 where ~80% of the neutral band has been removed; at this point, using the anion and neutral monomer extinction coefficients, there is one anion per 4.9 monomers of pF.

Smaller spectral changes do occur before the departure from linearity in Figure 4. The width of the NIR band, measured at the half-maximum, increases relative to the width of the earliest spectra. This half-width is 1.3 times larger in spectrum 5, in which ~53% of the neutral band has been removed.

With full removal of the pF neutral band (spectrum 7 in Figure 3), the width of the NIR band is ~2.2 times larger than the width during early reductions, and a high-energy tail extends into the visible region. The maximum has shifted from 0.5 to 0.57 eV, and structural features appear on the high-energy side of the band. Those features occur at spacings of ~1500 cm^{-1}, suggesting that they might be C═C vibrational spacings, but their origin is not clear. The features might alternatively be due to production of bipolarons[15−19,21,25] or to polarons confined and compressed in pF chains of different lengths, making a "polaron lattice".[16] At the same time, the absorbance at 2.07 eV (600 nm) has decreased and a new or substantially shifted band gives

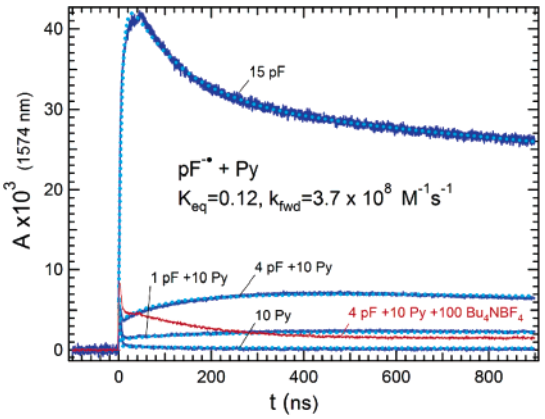

Figure 5. Reaction of $pF^{-\bullet}$ with pyrene in THF observed at 1574 nm where $pF^{-\bullet}$ absorbs well and pyrene$^{-\bullet}$ absorbs negligibly. The kinetic traces are labeled by concentrations in millimolars, using the monomer concentration for pF. Fits giving the rate and equilibrium constant, K_{eq} (in polymer concentration assuming $n = 11$), are shown as dashed lines through the data. A remarkable shift of the equilibrium occurs upon addition of 100 mM tetrabutylammonium tetrafluoroborate.

broad absorption from ~2.2 to 3.2 eV. On the basis of the extinction coefficient of the anion at 2480 nm, there is one anion for each ~3.2 repeat units, but the shift and broadening of this band suggest this assumption of a constant extinction coefficient may underestimate the number of anions. The actual extent of reduction at spectrum 7 is not known. The assumption that oscillator strength from 800 to 3000 nm is a better indication of the number of anions leads to the conclusion that there is one anion for each ~2 repeat units of the polymer. We conclude that at spectrum 7, where all neutral absorption has been removed, an average polymer having 11 repeat units holds between two and five negative charges, the larger number being more likely.

Bimolecular Charge Transfer in Solution: Redox Potentials. Cyclic voltammetry of pF in THF/0.1 M Bu_4NBF_4 produced broad waves from which accurate potentials could not be deduced, but accurate potentials can be obtained from reversible bimolecular charge transfer. $pF^{+\bullet}$ and $pF^{-\bullet}$ ions participate in bimolecular charge-transfer reactions with small molecules in solution. Those reactions often go to completion. Electron transfer from $pF^{-\bullet}$ to benzophenone (BzPh) or nitrobenzene (NBz) and hole transfer from $pF^{+\bullet}$ to ferrocene (Fc), quaterthiophene, or tri-*p*-tolylamine result in complete transfer of charge from the pF anions or cations. Similarly, bithiophene$^{-\bullet}$ ($2T^{-\bullet}$) transfers all its charge to pF (example kinetic traces are in Figures S-1 and S-2 shown in the Supporting Information). Reaction of $pF^{-\bullet}$ with pyrene does not go to completion, but to an equilibrium. The data at 1574 nm (Figure 5) give $K_{eq} = 0.12$ and $k_{fwd} = 3.7 \times 10^8$ M^{-1} s^{-1} for the reaction $pF^{-\bullet} + Py \rightleftharpoons pF + Py^{-\bullet}$ (pF concentrations in polymer units, assuming $n = 11$). Measurement at 600 nm gave identical values within 5%. The equilibrium constant increased by a factor of 21 in the presence of an electrolyte.

A similar equilibrium is observed for the reaction of $pF^{+\bullet}$ with terthiophene (3T) in DCE: $pF^{+\bullet} + 3T \rightleftharpoons pF + 3T^{+\bullet}$, yielding $K_{eq} = 1.34$ and $k_{fwd} = 3.9 \times 10^7$ M^{-1} s^{-1} (Figure S-3, Supporting Information).

Discussion

Polaron Nature of Positive and Negative Charges in Polyfluorene. Figures 1 and 2 show transient absorptions attributable to $pF^{+\bullet}$ and $pF^{-\bullet}$. From early in their formation (~1 ns) to >10 μs (>100 μs for $pF^{+\bullet}$), the principal features of the spectra remain the same indicating the presence of a single type of species: there are no noticeable shifts in the NIR bands, and the maxima of the visible bands remain constant to within a few percent.

Although the nature of charges in conjugated polymers has sometimes been debated,[14−19,21,25] the natures of "$pF^{+\bullet}$ and $pF^{-\bullet}$" observed here seem simple and clear: Holes in DCE or solvated electrons in THF attach to pF to inject single charges. Concentrations of ~1 μM holes or electrons in the solvent react with ~1−10 mM (monomer) or ~0.09−0.9 mM (polymer) pF; the >90:1 concentration ratio assures that one electron or hole is attached to a pF molecule, and attachment of two or more charges would be a very rare event. There is no doubt that the initial event is capture of single electrons or holes by pF molecules, but charges on different polymer chains might combine later to make bipolarons.

How much later? The combination of two $pF^{+\bullet}$ or $pF^{-\bullet}$ ions to make a bipolaron would require an encounter of two polymer chains, each containing a charge. The electron pulses employed in these experiments produced $pF^{+\bullet}$ or $pF^{-\bullet}$ ions in concentrations of 0.8−3 μM for the data in Figures 1 and 2. A maximum plausible estimate of the diffusion-controlled rate constant for such encounters between two charged pF molecules is 1×10^{10} M^{-1} s^{-1}, leading to a rate of 3×10^4 s^{-1} for such encounters. Clearly, the pF ions, most of which are formed within 50 ns (for $pF^{+\bullet}$) or 10 ns ($pF^{-\bullet}$) after the pulse, have no opportunity to become bipolarons for a much longer time. Further confirmation is provided by the bimolecular charge-transfer experiments which show that $pF^{+\bullet}$ and $pF^{-\bullet}$ are formed upon charge transfer from other singly charged molecular ions or transfer charge to other molecules to create well-known radical ions. The time-resolved experiments show decisively that the spectra in Figure 2 are due to single charges on polymer chains.

Polarons are expected to have two principal absorption bands at energies below that of the neutral[16,18,43] as observed in Figures 2 and 3. Figure 6 depicts single-electron pictures of optical transitions in neutral and negatively charged pFs. Addition of one electron to the LUMO of the neutral creates a singly occupied molecular orbital (SOMO), participating in two new transitions. A lower energy near-IR band of negative polarons is principally due to a SOMO → LUMO transition (P_1), whereas a visible band corresponds to HOMO → SOMO transition (P_2). There is another higher-energy UV band (P_3) which could overlap with the neutral HOMO → LUMO transition. These features were qualitatively reproduced in ZINDO/S calculations carried out for nonalkylated oligofluorenes ($n \leq 6$). For $pF^{+\bullet}$, one electron is removed from the neutral HOMO and HOMO → SOMO and SOMO → LUMO transitions contribute to two positive polaron bands.

$pF^{-\bullet}$ Polarons by Chemical Reduction with Na. The spectra formed in the early stages of reduction by metallic Na (Figure 3) are nearly identical to that of $pF^{-\bullet}$ formed by electron pulses.

(43) Skotheim, T. A. *Handbook of Conducting Polymers*, 2nd ed.; Marcel Dekker: New York, 1997.

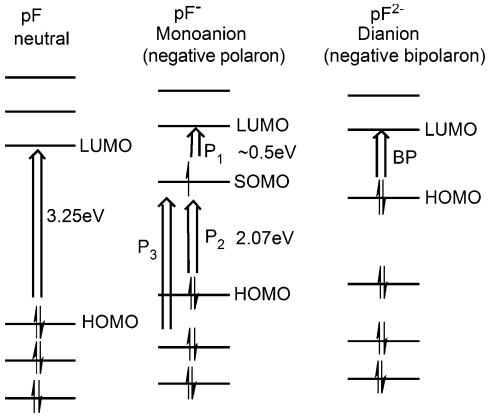

Figure 6. Principal contributions of optical transitions for, from left to right: neutral pF, a pF monoanion (negative polaron), and a pF dianion (negative bipolaron). In neutral molecules, the transition across the HOMO−LUMO gap is the lowest-energy transition. P_1, P_2, and P_3 denote NIR, vis, and UV (weak) polaron bands; P_2 is similar to the "across-the-gap" transition in the neutral pF, and for bipolarons, no such transition is possible. Instead, they have a single band in the visible region more akin to the NIR transition in polarons and can also have a weak UV band.

The only difference seen in the direct comparison (Figure 2) is a slight narrowing on the high-energy side of the 600 nm band. Chemically oxidized pF films (with $FeCl_3$) also showed similar spectral features at 0.75 and 2.1 eV.[44] We may therefore conclude that in reduction both by Na and by electron pulses the spectra are due to single $pF^{-\bullet}$ ions. The experiments are different in that the Na reductions, like other chemical reduction experiments, were performed on a time scale of several minutes, so despite the micromolar concentrations, there is ample time for two $pF^{-\bullet}$ ions to encounter each other to form bipolarons. That $pF^{-\bullet}$ is still formed tells us that, given the opportunity, bipolarons appear not to be formed under these conditions. Another difference is that the positive counterion to $pF^{-\bullet}$ is Na^+, which is unreactive toward $pF^{-\bullet}$. The counterion in the pulse radiolysis experiments is the solvated proton, RH_2^+. Reaction of protons with $pF^{-\bullet}$ leads to destruction of the anions, so any $pF^{-\bullet}$observed is almost certainly a free ion. The unreactivity of Na^+ enables observation on the minutes−hours time scale but leads to the possible formation of ion pairs ($pF^{-\bullet}$, Na^+). On the basis of known dissociation constants for ion pairs in THF,[45] single $pF^{-\bullet}$ ions are likely to be predominantly dissociated to free ions.

Delocalization Length, a Computational Question on the Nature of Polarons and Polaron Packing. The results in Figure 4 showed that creation of one $pF^{-\bullet}$ by Na reduction removed neutral absorption equivalent to the disappearance of 4.5 ± 0.5 monomer units. Figure 7 depicts an interpretation that a $pF^{-\bullet}$ occupies 4.5 contiguous monomer units, which is the delocalization length, l_n, of $pF^{-\bullet}$. A recent study has observed optical transitions in ions of oligomers of two to five fluorenes.[46] The reported trend shows a leveling out at $n = 4$ or 5, consistent with the delocalization length $l_n = 4.5$ reported here. Although the absorption maxima in solution appeared at ~0.7 eV for the lowest-energy (P_1) transitions of the longest oligomers, the corresponding transition was found at 0.5 eV for pF in the present study. The small difference (0.1−0.2 eV) between the polymer and the oligomer could be at least partly due to the longer conjugation length of the polymer. This is manifested in the difference in the HOMO−LUMO gap (of the neutral form) between the polymer (3.25 eV) and the oligomer (3.34−3.36 eV for the pentamer).

Wohlgenannt[47] argued that polarons are best characterized by their lengths in distance units. From the 0.85 nm length of a fluorene monomer, a $pF^{-\bullet}$ is 3.8 nm long. Wohlgenannt also reported a spectrum in solid films at 80 K, identified as "polarons", possibly $pF^{+\bullet}$ and $pF^{-\bullet}$; Wohlgenannt's[47] spectrum appears to be red-shifted from that in Figure 3, possibly due to the lack of relaxation in the frozen film. Although the length, $l_n = 4.5$ units, was obtained from the slope of Figure 4, it is also consistent with the departure from linearity at an average of one electron for each ~4.9 monomer units. A reasonable conclusion from these spectra is that the $l_n = 4.5$ polarons remain separate species whose properties change only moderately until sufficient electrons are added to force them to either overlap or compress (Figure 8) to shorter lengths.

An alternative to the picture of a charge in $pF^{-\bullet}$ as spread over ~4.5 adjacent monomer units emerged in a recent study of positive charges in fluorene oligomers, F_n. Using AM1 calculations, Goldsmith[13] reported that the highest occupied orbital of $F_4^{+\bullet}$ resides mainly on the two terminal fluorenes. From that result, one might infer a noncontiguous picture of the polaron. Reproducing the AM1u calculation on $F_4^{+\bullet}$, we confirmed the bifurcated orbital described by Goldsmith, but the charge and spin were both distributed almost evenly over the 4 fluorene units. A single orbital reflects the distribution of one electron, but many electron effects determine the charge distribution. In contrast to the AM1 result, other methods, INDOu or uB3LYP/3-21g, predicted that even the singly occupied orbital of $F_4^{+\bullet}$ is spread approximately evenly over contiguous units. Such differences among methods can be due to spin contamination, which was larger from AM1 than the other methods. Similar results were found for an AM1u on calculation of $F_4^{-\bullet}$. We conclude that there is no conflict with observations of Goldsmith[13] and that computation supports the picture of charges in conjugated polymers as polarons, which distribute charge over a few or several contiguous units as illustrated for an electron in $F_9^{-\bullet}$ in Figure 7. The contiguous picture proposed here also offers compatibility with observations during further reduction discussed below.

Upon further reduction, bipolaron formation is possible, which is expected[16,18,19,48] to remove the polaron bands and replace them with a single transition, labeled BP in Figure 6. Extensive reduction by Na injected one electron per each ~2 (possibly up to 4.5)[49] monomer units, placing ~five electrons in average-sized pF molecules having 11 monomers. Still, the polaron bands persisted (Figure 3, spectrum 7). Not only are polarons clearly the main species at low doping but also they appear to strongly resist pairing to form bipolarons (Figure 8). The broadening, shifts, and structure appearing in the polaron bands in spectra 6 and 7 in Figure 3 may be due to (a) ion pairing, where multiply

(44) Pogantsch, A.; Wenzl, F. P.; Scherf, U.; Grimsdale, A. C.; Mullen, K.; List, E. J. W. *J. Chem. Phys.* **2003**, *119*, 6904−6910.
(45) Slates, R. V.; Szwarc, M. *J. Phys. Chem.* **1965**, *69*, 4124−4131.
(46) Fratiloiu, S.; Grozema, F. C.; Koizumi, Y.; Seki, S.; Saeki, A.; Tagawa, S.; Dudek, S. P.; Siebbeles, L. D. A. *J. Phys. Chem. B* **2006**, *110*, 5984−5993.
(47) Wohlgenannt, M.; Jiang, X. M.; Vardeny, Z. V. *Phys. Rev. B* **2004**, *69*, 241204.
(48) Guay, J.; Kasai, P.; Diaz, A.; Wu, R. L.; Tour, J. M.; Dao, L. H. *Chem. Mater.* **1992**, *4*, 1097−1105.
(49) The larger number of charges giving one e^- per 2 monomer units is more probable, being consistent with the oscillator strength of the NIR band.

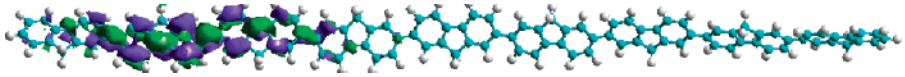

Figure 7. Pictorial representation of a polaron of an $F_9^{-\bullet}$ from the SOMO computed by Zindo1 on $F_9^{-\bullet}$ without alkyl chains.

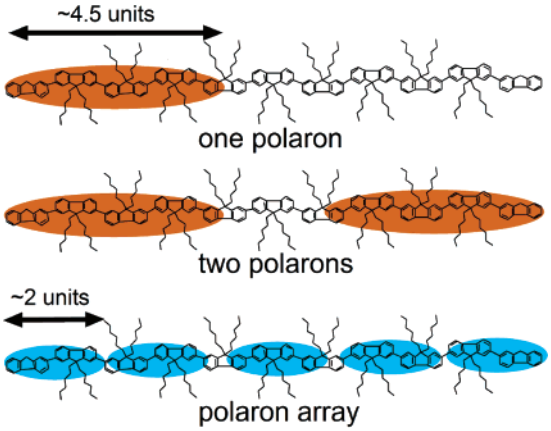

Figure 8. Schematic view of charge distributions (shaded ovals) in a single polaron, two polarons, and packed polarons ("polaron array" or "polaron lattice") in polyfluorene chains. Delocalization lengths of charges (~4.5 units in separate polarons) could be shortened upon extensive charge injections as illustrated for the polaron array. A pair of polarons is distinguished from the alternative picture of two charges sharing one geometrical distortion called a bipolaron.

charged anions are almost certainly paired with Na^+ which may produce blue shifts; (b) electronic interactions between adjacent polarons which may produce blue shifts;[18] and (c) compression of polarons, as illustrated in Figure 8 (bottom), which probably occurs given the finding that charges occupy as few as 2 repeat units with extensive reduction. Evidence for compressed polarons could be consistent with a "polaron lattice",[16] but this concept is not clearly tested by the present data. A striking feature is the large alteration of the visible (600 nm) band in spectrum 7 of Figure 3. It is plausible that interactions between adjacent polarons lead to a large change in the excited state for this high-energy band.

Redox Potentials and Exciton Binding Energy for pF. Table 2 summarizes energetics for formation of $pF^{+\bullet}$ and $pF^{-\bullet}$. The equilibria and redox potentials observed by electrochemical measurements on the reference molecules, terthiophene (3T) and pyrene (Py), yielded the redox potentials $E°(pF^{+/0})$ and $E°(pF^{0/-})$ in 0.1 M Bu_4NBF_4. Potentials are reported against a ferrocene/ferrocenium reference in each solvent, $E°(Fc^{+/0})$. Table 2 also compares the values measured here to determinations on pF films, in acetonitrile by Janietz et al.,[22] and pF end capped by amines, in CH_2Cl_2 by Miteva et al.,[23] both containing 0.1 M Bu_4NBF_4. Our $E°(pF^{+/0})$ value is closer to Miteva's value, and our $E°(pF^{0/-})$ value is closer to Janietz's value. We note that the present experiments obtain entirely reversible thermodynamic values in solutions with or without an electrolyte. Irreversibilities found in previous cyclic voltammetry studies would be likely to cause deviations from the values reported here. The present experiments definitely observe one-electron redox processes. The electrochemical measurements almost certainly add multiple charges, analogous to the multiple electron additions seen here by Na reduction (Figure 3). Multiple reductions/oxidations may broaden and shift the voltammograms.

The data presented here provide useful insights into charge injection barriers in wire-donor and wire-acceptor architectures and also in OLED devices. Ultraviolet photoelectron spectroscopy (UPS) has been used to obtain the ionization potential (IP) of pF films (IP $\sim$ 5.8 $\pm$ 0.1 eV)[20,21,50] and to estimate the electron affinity (EA $\sim$ 2.6 eV) by subtracting the optical gap.[50] The bulk pF IP is in reasonable agreement with our single-electron redox potential.

The energetics of polaron formation established here also provides useful information for understanding photoexcitation of pF. The difference of these gives the free energy, to form separated $pF^{+\bullet}$ and $pF^{-\bullet}$ ions, of 3.31 eV. Figure 9 summarizes the energetics for photoexcited pF. Energies of the excited singlet and triplet states of pF are 3.1 $\pm$ 0.1 (average of four values)[28,51,52] and 2.3 eV.[51] The exciton binding energy for singlet excited states is then 0.2 eV in solution in the presence of 0.1 M Bu_4NBF_4. Photoexcitation of conjugated polymers is typically carried out in a less polar environment. Although the present experiments also measure equilibria without an electrolyte, reference redox potentials without an electrolyte are not accurately known. Estimates of solvation free energies can be made from redox potentials, ionization potentials, and electron affinities.[53] Applying similar methods to pyrene, we obtain 3.43 eV for the sum of differential (difference between the ion and the neutral) solvation energies for $pyrene^{+\cdot}$ and $pyrene^{-\cdot}$. Although not highly reliable, estimates of the effect of polarity on solvation energies and therefore redox potentials can be made using the Born equation,[54] $\Delta G_s = -e^2(1 - 1/\epsilon_s)/2r_{Born}$, where ϵ_s is the static dielectric constant. Estimates utilizing this Born dielectric continuum approach, described in more detail in the Supporting Information accompanying this article, predict that in THF $\epsilon_s = 7.6$ without an electrolyte, the magnitudes of solvation free energies for a pair of pyrene anions and cations would be smaller by 0.29 eV relative to average solvation energies under electrochemical conditions (~0.1 M electrolyte) in THF or by 0.40 eV in acetonitrile with an electrolyte. With this estimate, data in Table 2 predict that the free energy to form separated $pF^{+\bullet}$ and $pF^{-\bullet}$ ions in THF would increase from 3.31 eV in the presence of an electrolyte to ~3.44 eV in its absence. If the effective dielectric constant in a polymer film was ~3−4,[55] then the free energy to create $pF^{+\bullet}$ and $pF^{-\bullet}$ ions (in the solid state) might increase to ~3.6−3.8 eV, giving exciton binding energies, E_b, of ~0.5−0.7 eV in the solid state. This is only a rough estimate because it relies on the Born equation and because it is very sensitive to the dielectric constant, which is known only approximately. A better estimate would require a better understanding of solvation energies of ions. Alvarado[56] determined a lower value, $E_b = 0.3$ eV, in polymer films, by voltage-resolved STM, but later work by the

(50) Hwang, J.; Kahn, A. *J. Appl. Phys.* **2005**, *97*, 103705.
(51) Monkman, A. P.; Burrows, H. D.; Hartwell, L. J.; Horsburgh, L. E.; Hamblett, I.; Navaratnam, S. *Phys. Rev. Lett.* **2001**, *86*, 1358−1361.
(52) Koizumi, Y.; Seki, S.; Acharya, A.; Saeki, A.; Tagawa, S. *Chem. Lett.* **2004**, *33*, 1290−1291. Jo, J. H.; Chi, C. Y.; Hoger, S.; Wegner, G.; Yoon, D. Y. *Chem.−Eur. J.* **2004**, *10*, 2681−2688.
(53) Case, B.; Hush, N. S.; Parsons, R.; Peover, M. E. *J. Electroanal. Chem.* **1965**, *10*, 360−370.
(54) Born, M. *Z. Phys.* **1945**, *1*, 45.
(55) Karg, S.; Dyakonov, V.; Meier, M.; Riess, W.; Paasch, G. *Synth. Met.* **1994**, *67*, 165−168. Blom, P. W. M.; deJong, M. J. M.; vanMunster, M. G. *Phys. Rev. B* **1997**, *55*, R656−R659.
(56) Alvarado, S. F.; Seidler, P. F.; Lidzey, D. G.; Bradley, D. D. C. *Phys. Rev. Lett.* **1998**, *81*, 1082−1085.

Table 2. Redox Potentials (V vs $Fc^{+/0}$) of Poly-2,7-(9,9-dihexylfluorene) (pF, $n \sim 11$) from Charge-Transfer Equilibria[a]

		polymer, $n = 11$		E^0 vs $Fc^{+/0}$ (V)		
reaction	solvent	K_{eq}	$\Delta G°$ (±5 meV)	ref Mol	E^0(pF)	other E^0(pF) reports
$pF^{+\bullet} + 3T$	DCE	1.34	−7.4			
$pF^{+\bullet} + 3T$	DCE + 0.1 M Bu_4NBF_4	27[b]	−85	0.57[c]	0.66	+0.97 to +1.07,[22] +0.73[23]
$pF^{-\bullet} + Py$	THF	0.12	54			
$pF^{-\bullet} + Py$	THF + 0.1 M Bu_4NBF_4	2.5	−24	−2.63[d]	−2.65	−2.7 to −2.8,[22] −2.1 to −2.3[23]
$\Delta G°$ (2pF → $pF^{+\bullet} + pF^{-\bullet}$) in 0.1 M Bu_4NBF_4 (eV)[e]					3.31	

[a] $E^0(pF^{+/0}) = E^0(\text{ref}) - \Delta G°$ and $E^0(pF^{0/-}) = E^0(\text{ref}) + \Delta G°$, where E^0(ref) is the reversible electrochemical potential of a reference molecule (terthiophene, 3T, or pyrene, Py). Also given is the free energy for formation of a pair of positive and negative pF polarons, $\Delta G°$ (2pF → $pF^{+\bullet} + pF^{-\bullet}$). [b] The equilibrium constant in DCE was assumed to increase by a factor of 21 upon addition of an electrolyte as found for anions. [c] Ref 25 gives $E^0(3T^{+/0}) = +0.95$ V vs Ag/AgCl. Corrected for ferrocene, $Fc^{+/0}$, using $E^0(Fc^{+/0}) = +0.38$ V.[63] [d] $E^0(Py^{0/-})$ in THF + 0.1 M Bu_4NBF_4 measured in this work. [e] Free-energy change for the formation of ions at infinite distance with a 0.1 M electrolyte in a solvent such as THF or DCE. The energetics are likely to be very similar in a more polar solvent.

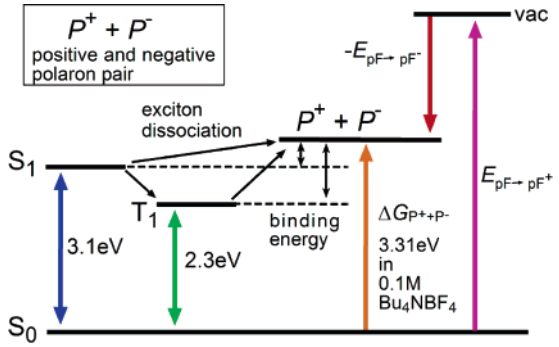

Figure 9. Energetics of optical excitation in pF in a solvent containing an electrolyte, evaluating the exciton binding energy.

same and other authors showed that image forces and aggregates[57,58] lead to variations for the true band gap. For ladder PPP, the value free of these effects was reported to be $E_b = 0.8$ eV;[58] so the very rough estimate given here for films might be plausible.

The experimental information described here places the dissociated polaron pair, $pF^{+\bullet}$ and $pF^{-\bullet}$, above the excited S_1 singlet (exciton) state. Femtosecond laser excitation produces the (S_1) state,[7,59−61] which exhibits fast conformational relaxation.[61] Excitation above the exciton state could produce transient, separated $pF^{+\bullet}$ and $pF^{-\bullet}$. After the fast conformation changes,[61] a signature for production of $pF^{+\bullet}$ and $pF^{-\bullet}$ should be a spectrum equal to the sum of the $pF^{+\bullet}$ and $pF^{-\bullet}$ spectra in Figure 3: there should be a sharp visible band near 590 nm and a strong NIR band. Xu reported that high excitation intensities yield a state above S_1, tentatively identified with dissociated $pF^{+\bullet}$ and $pF^{-\bullet}$.[7,59,60] This state displayed a broad transient absorption and delayed fluorescence with a lifetime of ∼300 ps, but the broad absorption spectrum reported for that state[59] bears almost no resemblance to the much sharper absorptions for $pF^{+\bullet}$ and $pF^{-\bullet}$ reported here; Xu's ∼300 ps state is probably *not* a weakly interacting, dissociated, or nearly dissociated $pF^{+\bullet}$ and $pF^{-\bullet}$ pair. Polaron pairs, having character intermediate between "molecular excitations and free charge carriers", might exist and have finite lifetimes[10] and have been discussed in conjugated polymers.[8,62] For pF, the absorption signature of separated $pF^{+\bullet}$ and $pF^{-\bullet}$ is established here.

Conclusions

A conjugated polymer poly-2,7-(9,9-dihexylfluorene) (pF) with an average length of ∼10.9 fluorene units was synthesized. Charge attachments to pF dissolved in organic solvents were studied by pulse radiolysis. Nonexponential kinetics of diffusion-controlled charge attachment to long molecules was seen due to large transient terms as previously reported for other conjugated polymers. Transient absorption spectra of positively and negatively charged pF were very similar. Monocations of pF generated in 1,2-dichloroethane (DCE) showed a peak at 580 nm, and monoanions in tetrahydrofuran (THF) showed a peak at 600 nm; both ions had strong absorption bands in the near-infrared region. Comparisons with known molecular ions established the absorption coefficients of both pF anions and cations. Chemical reductions of pF were carried out using metallic sodium as a reducing agent. At early stages of sodium doping, the spectra resembled those of radiolytically generated ions, showing absorption bands at 600 and 2480 nm. Difference absorption spectra of growing anions and bleaching of the neutral band at 380 nm permitted estimation of the delocalization length of polarons to be ∼4.5 fluorene units. The extent of charge distribution was roughly reproduced by the SOMO orbital obtained with ZINDO1 calculations on a model oligomer with 9 fluorene units. Chemical reduction experiments also revealed the persistence of polaron bands after injection of ∼2 charges per chain indicating that dominant charge carriers in pF are singly charged polarons, not doubly charged bipolarons. More extensive reduction by sodium compressed the polarons to occupy as few as 2−3.2 fluorene units. Still, two polaron bands remained, although they were blue-shifted and broadened, and possibly, a periodic structure appeared on the near-infrared band.

Redox equilibria of excess electrons between pF and pyrene as well as those of excess holes between pF and terthiophene were observed by pulse radiolysis. The presence of a supporting electrolyte was found to shift the equilibria toward the small molecules. Using the equilibrium constants obtained, reversible one-electron reduction potentials were determined as $E^0(pF^{+/0}) = +0.66$ V vs $Fc^{+/0}$ in DCE and as $E^0(pF^{0/-}) = -2.65$ V vs $Fc^{+/0}$ in THF. The results also allowed us to estimate the exciton

(57) Rossi, L.; Alvarado, S. F.; Riess, W.; Schrader, S.; Lidzey, D. G.; Bradley, D. D. C. *Synth. Met.* **2000**, *111*, 527−530. Sigaud, P.; Chazalviel, J. N.; Ozanam, F.; Stephan, O. *J. Appl. Phys.* **2001**, *89*, 466−470.
(58) Alvarado, S. F.; Barth, S.; Bussler, H.; Scherf, U.; van der Horst, J. W.; Bobbert, P. A.; Michels, M. A. J. *Adv. Funct. Mater.* **2002**, *12*, 117−122.
(59) Xu, Q. H.; Moses, D.; Heeger, A. J. *Phys. Rev. B* **2004**, *69*, Art. No. 113314.
(60) Xu, Q. H.; Moses, D.; Heeger, A. J. *Phys. Rev. B* **2003**, *68*, Art. No. 174303.
(61) Dias, F. B.; Macanita, A. L.; de Melo, J. S.; Burrows, H. D.; Guntner, R.; Scherf, U.; Monkman, A. P. *J. Chem. Phys.* **2003**, *118*, 7119−7126.
(62) Schindler, F.; Lupton, J. M.; Muller, J.; Feldmann, J.; Scherf, U. *Nat. Mater.* **2006**, *5*, 141−146.
(63) Smie, A.; Synowczyk, A.; Heinze, J.; Alle, R.; Tschuncky, P.; Gotz, G.; Bauerle, P. *J. Electroanal. Chem.* **1998**, *452*, 87−95.

binding energies in pF to be ~0.2 eV for a singlet exciton in the presence of 0.1 M Bu_4NBF_4.

Information about the spatial extent of charge carriers (sizes of polarons) as well as detailed energetics of charge injection obtained from the present study would be useful for further developments of polyfluorenes and other conjugated polymers in electronic and energy conversion devices.

Experimental Details

Pulse Radiolysis. For polymer solutions, the concentration of repeat units used was typically around 0.2−10 mM. The monitoring light source was a 75 W Osram pulsed xenon arc lamp pulsed to a few hundred times its normal intensity. Wavelengths were selected using either 40 or 10 nm interference filters. Transient absorption signals were detected with an FND-100Q (EG&G) silicon (≤1000 nm, 2 ns rise time) diode, a GEP-600L (Germanium Power Devices) germanium diode (6 ns), or a SU500 (Sensors Unlimited) InGaAs (≥1500 nm, 8 ns) diode and digitized with a Tektronix TDS-680B or 694C oscilloscope. When a faster rise time was needed (e.g., Figure 1b), a Hamamatsu R-1328u-03 biplanar phototube was employed giving an overall system rise time of 0.2 ns. Solid-state photodiodes typically have bi- or multistage response times near their band edges.[64] At wavelengths of 950 nm and shorter, FND100Q exhibits a simple 2 ns rise time, but at 1000 nm, 15% of the response has a slower, ~60 ns, rise. The GEP-600L used at 1000−1628 nm has a similar anomaly throughout its wavelength range, with increased rise near its band edge (e.g., 400 ns, ~20% at 1574 nm). For the InGaAs, the delayed component reaches 45% with $\tau_{10-90} = 0.93\ \mu$s. Measurements of rates reported herein were all obtained at wavelengths where the InGaAs detector was not needed and were unperturbed or only mildly perturbed by these secondary responses. Any uncorrected effects are included in reported uncertainties, which are ±15% unless reported otherwise. Spectra showed these effects at times <1 μs; reported here are spectra at sufficiently long times that effects of detector responses were small.

The transmission/time data were analyzed with Igor Pro software (Wavemetrics). Reaction rate constants were determined using a nonlinear least-squares fitting procedure described previously.[65] This procedure accounts for geminate recombination, which is encountered on the time scales investigated. Bimolecular rate constants were determined using the linearity of the observed pseudo-first-order growth of the product with respect to the solute concentration. Where not stated, uncertainties are 15%.

The total dose per pulse was determined before each series of experiments by measuring the change in absorbance of the electron in water. The dose received was calculated using ϵ (700 nm, e_{aq}^-) = 18830 M^{-1} cm^{-1} and $G(e_{aq}^-) = 2.97$. The dose was corrected for the difference in electron density of the organic solvents used compared to that of water. Radiolytic doses of 5−18 Gy were employed. Solutions in THF were prepared in an argon environment and sealed under argon with Teflon vacuum stopcocks. During irradiation, samples were exposed to as little UV light as possible to avoid photodecomposition, although no evidence of this occurring was found within the time frames monitored. Measurements were carried out at 22 ± 2° C.

UV−Vis−NIR Absorption Spectroscopy. Absorption spectra of pFs in THF and DCE had peaks corresponding to HOMO−LUMO transitions at 382 and 383 nm, respectively. Concentrations in the range of 50−400 μM (monomer unit concentrations using the formula weight 332.53) obeyed Beer's law yielding $\epsilon_{382} = 3.4 \times 10^4$ M^{-1} cm^{-1} in THF and $\epsilon_{383} = 2.9 \times 10^4$ M^{-1} cm^{-1} in DCE.

Reduction of pF was performed by successive contacts of the THF solution with sodium metal under a vacuum in a glass apparatus equipped with a 1 mm Infrasil quartz cell (Starna Cells, Inc.) connected to four arms. Sodium (Aldrich) was purified by distillation under a vacuum to form a metallic film inside the one arm. In another arm, the solution of pF (~0.14 mM) was prepared by vacuum transferring distilled THF from a NaK alloy onto pF. The absorption spectrum of the neutral served as a baseline for the subsequent measurements, providing subtraction of near IR absorptions due to vibrational overtones and combination bands of the solvent, THF. Some noise remained sometimes near the positions of the large changes in these solvent bands.

Acknowledgment. This work was supported by the U.S. Department of Energy, Office of Basic Energy Sciences, Division of Chemical Sciences, under Contract DE-AC02-98-CH10886. We thank James Wishart, Andrew Cook, Steve Howell, and Jack Preses at LEAF and Etsuko Fujita for technical advice and help in sodium reduction and electrochemical experiments.

Supporting Information Available: Transient absorption traces for charge transfer from $2T^{-\bullet}$ to pF and from $pF^{-\bullet}$ to BzPh and NBz in THF and charge-transfer equilibria between $pF^{+\bullet}$ and 3T in DCE (PDF). This material is available free of charge via the Internet at http://pubs.acs.org.

JA062596H

(64) Klassen, N. V.; Gillis, H. A.; Walker, D. C. *J. Chem. Phys.* **1971**, *55*, 1979−1980. Cline, J. A.; Jonah, C. D.; Bartels, D. M. *Rev. Sci. Instrum.* **2002**, *73*, 3908−3915.

(65) Miller, J. R.; Penfield, K.; Johnson, M.; Closs, G.; Green, N. In *Photochemistry and Radiation Chemistry. Complementary Methods for the Study of Electron Transfer*; Wishart, J. F., Nocera, D. G., Eds.; American Chemical Society: Washington D.C., 1998; Vol. 254, pp 161−176.